A Novel Dynein Light Intermediate Chain Colocalizes with the Retrograde Motor for Intraflagellar Transport at Sites of Axoneme Assembly in *Chlamydomonas* and Mammalian Cells

Catherine A. Perrone,* Douglas Tritschler,* Patrick Taulman,†
Raqual Bower,* Bradley K. Yoder,† and Mary E. Porter*‡

*Department of Genetics, Cell Biology, and Development, University of Minnesota, Minneapolis, Minnesota 55455; and †Department of Cell Biology, University of Alabama at Birmingham Medical Center, Birmingham, Alabama 35294

The assembly of cilia and flagella depends on bidirectional intraflagellar transport (IFT). Anterograde IFT is driven by kinesin II, whereas retrograde IFT requires cytoplasmic dynein 1b (cDHC1b). Little is known about how cDHC1b interacts with its cargoes or how it is regulated. Recent work identified a novel dynein light intermediate chain (D2LIC) that colocalized with the mammalian cDHC1b homolog DHC2 in the centrosomal region of cultured cells. To see whether the LIC might play a role in IFT, we characterized the gene encoding the *Chlamydomonas* homolog of D2LIC and found its expression is up-regulated in response to deflagellation. We show that the LIC subunit copurifies with cDHC1b during flagellar isolation, dynein extraction, sucrose density centrifugation, and immunoprecipitation. Immunocytochemistry reveals that the LIC colocalizes with cDHC1b in the basal body region and along the length of flagella in wild-type cells. Localization of the complex is altered in a collection of retrograde IFT and length control mutants, which suggests that the affected gene products directly or indirectly regulate cDHC1b activity. The mammalian DHC2 and D2LIC also colocalize in the apical cytoplasm and axonemes of ciliated epithelia in the lung, brain, and efferent duct. These studies, together with the identification of an LIC mutation, *xbx-1(ok279)*, which disrupts retrograde IFT in *Caenorhabditis elegans*, indicate that the novel LIC is a component of the cDHC1b/DHC2 retrograde IFT motor in a variety of organisms.

INTRODUCTION

Cilia and flagella are microtubule-based organelles that play critical roles in the fertility and viability of eucaryotic organisms. Defects in components required for flagellar assembly or motility can have profound consequences. In vertebrates,

    Abbreviations used: BAC, bacterial artificial chromosome; DHC, dynein heavy chain; D2LIC, light intermediate chain associated with mammalian DHC2; IC, intermediate chain; IFT, intraflagellar transport; LC, light chain; LIC, light intermediate chain; PBS, phosphate-buffered saline; RFLP, restriction fragment length polymorphism; RT-PCR, reverse transcription-polymerase chain reaction.

these include birth defects, the development of left-right asymmetries, respiratory distress, polycystic kidney disease, and male sterility (Nonaka *et al.*, 1998; Marszalek *et al.*, 1999; Afzelius, 1999; Murcia *et al.*, 2000; Pazour *et al.*, 2000; Yoder *et al.*, 2002). The polypeptide complexity of the organelles has made it challenging to analyze these structures in vertebrate tissues, but studies in model organisms such as *Chlamydomonas* and *Caenorhabditis elegans* have provided significant insights into the identity of components required for flagellar assembly and motility. Indeed, recent work has shown that both the assembly and maintenance of cilia and flagella are dependent on a bidirectional, intraflagellar transport system (IFT) (reviewed in Rosenbaum *et al.*, 1999; Sloboda, 2002). Anterograde transport (from the cell body to the tip of the flagellum) requires a heterotrimeric kinesin (Kozminski *et al.*, 1995; Piperno and Mead, 1997; Cole *et al.*, 1998), whereas retrograde transport (from the flagellar tip to the cell body) depends on an unusual class of cytoplasmic

Table 1. Characteristics of strains used in this study

Strain name	Phenotype	References
wt (*CC-125*)		
pf28 (CC-1877)	Lacks outer dynein arms	Mitchell and Rosenbaum (1985)
E8 (*pf9 pf28* suppressed) (*CC-3903*)	Lacks outer dynein arms and I1 inner arm dynein	Porter *et al.* (1992)
fla14 (V64) (CC-3937)	Short flagella, lacks retrograde IFT, *LC8* null	Pazour *et al.* (1998)
fla15 (CC-3861)	ts, decreased retrograde IFT	Piperno *et al.* (1998); Iomini *et al.* (2001)
fla16 (CC-3862)	ts, decreased retrograde IFT	Piperno *et al.* (1998); Iomini *et al.* (2001)
fla17 (CC-3863)	ts, decreased retrograde IFT	Piperno *et al.* (1998); Iomini *et al.* (2001)
lf1-1 (CC-802)	Long flagella	McVittie (1972); Barsel *et al.* (1988)
lf2-1 (CC-803)	Long flagella	McVittie (1972); Barsel *et al.* (1988)
lf3-2 (CC-2289)	Long flagella	Barsel *et al.* (1988)
stf1-1 (CC-3915)	Stumpy flagella, *cDhc1b* null	Porter *et al.* (1999)
stf1-2 (CC-3916)	Stumpy flagella, *cDhc1b* null	Porter *et al.* (1999)

dynein known as cDHC1b (Pazour *et al.*, 1999; Porter *et al.*, 1999; Signor *et al.*, 1999a; Wicks *et al.*, 2000).

The heterotrimeric kinesins have been characterized in several organisms (Cole *et al.*, 1993, 1998; Yamazaki *et al.*, 1995; Signor *et al.*, 1999b), but relatively little is known about the cDHC1b class of motors. (The cDHC1b sequence is known by multiple names in different organisms. For simplicity, we will refer to the mammalian sequence as DHC2, and the *Chlamydomonas* and *C. elegans* sequences as cDHC1b). *cDHC1b* was first identified in sea urchin embryos as a sequence that is closely related to the major cytoplasmic dynein but whose expression could be stimulated by deciliation, similar to the axonemal dyneins (Gibbons *et al.*, 1994). Subsequent studies in mammalian cells identified the homologous sequence, *DHC2*, in a variety of cells and tissues, but this transcript was most abundant in ciliated cells (Tanaka *et al.*, 1995; Criswell *et al.*, 1996; Vaisberg *et al.*, 1996; Neesen *et al.*, 1997; Criswell and Asai, 1998). Immunolocalization studies indicated an enrichment of DHC2 in the apical cytoplasm of isolated tracheal epithelial cells (Criswell *et al.*, 1996). However, DHC2 was also found in close association with the Golgi apparatus in tissue culture cells, where it was proposed to be involved in some aspect of membrane trafficking (Vaisberg *et al.*, 1996).

The identification and characterization of *cDhc1b* mutants in *Chlamydomonas* (Pazour *et al.*, 1999; Porter *et al.*, 1999) and *C. elegans* (Signor *et al.*, 1999a; Wicks *et al.*, 2000) revealed that cDHC1b is essential for flagellar and ciliary assembly and retrograde IFT, but little was known about the identity of other components of the motor complex. Mutations in a dynein light chain, LC8, are associated with defects in retrograde IFT in *Chlamydomonas* (Pazour *et al.*, 1998). Although LC8 is a component of several different axonemal complexes, no direct association with the cDHC1b motor has yet been demonstrated. On the other hand, recent work in mammalian cells has identified a novel dynein light intermediate chain, D2LIC, that is related to the LICs associated with the conventional cytoplasmic dynein (cDHC1a). However, D2LIC associates exclusively with DHC2 by biochemical criteria and by immunofluorescence (Grissom *et al.*, 2002). The mammalian D2LIC protein is also abundant in ciliated tissues, suggesting that it too might play a role in IFT and flagellar assembly.

To address the potential role of this novel LIC in flagellar assembly, we have analyzed the cDHC1b complex in *Chlamydomonas*, and we have characterized the subcellular localization of the novel LIC in both *Chlamydomonas* cells and mammalian tissues. In this report, we present evidence that the novel LIC is an integral component of the cDHC1b complex in *Chlamydomonas*. In addition, we find that the cDHC1b/LIC complex is intimately associated with other IFT components in both *Chlamydomonas* and mammalian cells. Finally, we show that the distribution of the cDHC1b/LIC complex is significantly altered in a group of length control mutants, consistent with a central role of this complex in the regulation of both flagellar assembly and flagellar length. These results, together with the observation that mutations in the *C. elegans LIC* gene, *xbx-1*, disrupt the formation of sensory cilia in the worm (Schafer *et al.*, 2003), suggest that the role of the cDHC1b/LIC complex as the retrograde motor for IFT is conserved throughout ciliated organisms.

MATERIALS AND METHODS

Cell Culture and Mutant Strains

The strains listed in Table 1 were maintained as described previously (Porter *et al.*, 1999; Perrone *et al.*, 2000). *fla14* was provided by G. Pazour (University of Massachusetts Medical School, Worcester, MA); *fla15–fla17* were provided by G. Piperno (Mt. Sinai Medical School, New York, NY), and *stf1-1* and *stf1-2* were provided by W. Dentler (University of Kansas, Lawrence, KS). Other strains were either generated in this laboratory or obtained from the *Chlamydomonas* Genetics Center (Duke University, Durham, NC).

Characterization of the Full-Length cDHC1b Gene

Previous work had resulted in the recovery of ~14.5 kb of the *cDHC1b* transcription unit encoding ~70% of the polypeptide sequence (Porter *et al.*, 1999). To isolate the rest of the gene, a reverse transcription-polymerase chain reaction (RT-PCR) product derived from the 3′ end of the known sequence was used to screen a *Chlamydomonas* bacterial artificial chromosome (BAC) library (Genome Systems, St. Louis, MO) and recover two BAC clones (28d8 and 36o11). A 7.5-kb *Bam*HI/*Hin*dIII fragment was subcloned from BAC 28d8 and sequenced by primer walking. Potential open reading frames and splice sites were confirmed by sequence analysis of RT-PCR products (Myster *et al.*, 1999; Porter *et al.*, 1999; Perrone *et*

al., 2000). The full-length gene encodes a polypeptide of 4333 amino acids (aa) with a molecular mass of 481,430 daltons (accession number AJ132478).

Characterization of the LIC Gene

A search of the extended sequence tag (EST) database identified a *Chlamydomonas* EST (AW758232) with limited similarity to the amino terminus of the human D2LIC sequence. The EST sequence was recovered by RT-PCR and used to obtain BAC clones 38n5, 22e7, 37p12, 18l1, and 1o10. The complete LIC transcription unit was identified within an ~9-kb *Sac*I fragment from BAC clone 18l1. A full-length cDNA was recovered by screening a mixed *Chlamydomonas* cDNA library (*Chlamydomonas* Genetics Center) with the PCR product and an ~1-kb *Xho*I fragment derived from 3' end of the genomic clone (accession number AY157841).

Southern and Northern Blot Analyses and Restriction Fragment Length Polypmorphism (RFLP) Mapping

DNA and RNA isolation, restriction enzyme digests, agarose gels, Southern blots, and Northern blots were performed as described previously (Perrone *et al.*, 2000). To place the *LIC* gene on the genetic map, the RT-PCR product was used to identify a *Pvu*II RFLP between two *Chlamydomonas* strains, 137c and S1-D2. The *LIC* probe was then hybridized to a series of mapping filters containing *Pvu*II digested genomic DNA isolated from tetrad progeny of crosses between multiply marked *Chlamydomonas reinhardtii* strains and S1-D2. The segregation of the *LIC* RFLP was analyzed relative to the segregation of >42 genetic and molecular markers as described in Porter *et al.* (1996). *LIC* is linked to the genetic marker *sr1* (parental ditype:nonparental ditype:tetratype = 9:1:9, ~39 cM) and the molecular marker *NIT1* (parental ditype:nonparental ditype:tetratype = 14:0:12, ~23 cM).

Preparation of Antibodies against cDHC1b and LIC Fusion Proteins

Two cDHC1b fusion proteins were generated by cloning an ~1.6-kb RT-PCR product encoding residues 563–926 of the cDHC1b sequence into either pET5 (Novagen, Madison, WI) or pGEX (Pharmacia, Peapack, NJ) The primers for RT-PCR were designed from nucleotides 5392–5410 and 7020–7038 of the *cDHC1b* genomic sequence (AJ132478). TTA was added to the 5' end of the reverse primer to create an in-frame stop codon. The RT-PCR product was cloned into the pGEM-T Easy vector (Promega, Madison, WI), released by *Eco*RI digestion, and then subcloned into pET5a containing a 6x-His tag or pGEX-1 containing a glutathione *S*-transferase (GST) tag. The insoluble, 6xHis-tagged cDHC1b fusion protein was isolated from purified inclusion bodies by SDS-PAGE, equilibrated with phosphate-buffered saline (PBS), and used to immunize three rabbits (Covance, Richmond, CA). Anti-cDHC1b antibodies were affinity purified against the soluble GST-cDHC1b fusion protein that had been covalently cross-linked to a glutathione-Sepharose 4B column (Amersham Biosciences, Piscataway, NJ).

Two LIC fusion proteins were generated by cloning an ~1.1-kb PCR product encoding residues 1–371 of the LIC sequence into either pET30a or pGEX-2T. A *Bam*HI site was added to the forward primer, and a stop codon and *Hin*dIII site was added to the reverse primer. The PCR product was ligated into pGEM-T Easy and then released by digestion with either *Bam*HI/*Hin*dIII for cloning into pET30a or with *Bam*HI/*Eco*RI for cloning into pGEX-2T. The soluble 6xHis-LIC fusion protein was purified on a nickel column and injected into three rabbits (Covance), and antibodies were affinity purified against a soluble GST-LIC fusion protein as described above.

Protein Isolation, Immunoprecipitation, and Western Blotting

Large-scale culture of vegetative cells, the isolation and extraction of flagella, and sucrose density centrifugation of dynein extracts were performed as described in Porter *et al.* (1992) and Perrone *et al.* (2000). FPLC ion-exchange chromatography was performed as described in Gardner *et al.* (1994) and Myster *et al.* (1997). Immunoprecipitates were prepared from dynein extracts by using affinity-purified antibodies to the LIC. An affinity-purified antibody to the *Dhc10* gene product (Perrone *et al.*, 2000) served as a control for the immunoprecipitation reaction. Immunoprecipitation was performed with protein A-Sepharose by using standard protocols (Bonifacino *et al.*, 1999).

Polypeptides were separated by SDS-PAGE on 5–15% or 5–20% polyacrylamide, 0–0.25 M glycerol gradient gels and then blotted to polyvinylidene difluoride. Western blots were probed as described previously (Perrone *et al.*, 1998, 2000) using either mouse monoclonal antibodies to the p172, p139, or p81 IFT subunits (Cole *et al.*, 1998), rabbit polyclonal antibodies to FLA10 kinesin (Cole *et al.* 1998), dynein LC8 (R4058, King and Patel-King, 1995; King *et al.*, 1996), or the *DHC10* gene product (Perrone *et al.*, 2000), or the antibodies described above.

Immunofluorescence Light Microscopy

Chlamydomonas cells were processed for immunofluorescence microscopy by using the cold methanol fixation procedure of Sanders and Salisbury (1995). The affinity-purified LIC antibody was used at 1 μg/ml. The affinity-purified cDHC1b antibody at 50 μg/ml was pretreated with aliquots of methanol-fixed, *cDhc1b* mutant cells to reduce background staining and then used at a dilution of 1:10. Alexafluor-488 labeled, secondary antibodies (goat anti-mouse IgG or goat anti-rabbit IgG) were obtained from Molecular Probes (Eugene, OR) and diluted 1:400 in blocking buffer. Slides were washed in three changes of PBS and then mounted in Prolong antifade medium (Molecular Probes). Images were obtained using an Axiovert S100 TV microscope (Carl Zeiss, Thornwood, NY) and a Spot RT monochrome camera and imaging software (Diagnostics Instruments, Sterling Heights, MI).

Polarized cultures of Madin-Darby canine kidney (MDCK) cells grown on Transwell filters and tissues isolated from wild-type mice were prepared for immunofluorescence as described in Taulman *et al.* (2001). Primary antibodies used included rabbit anti-DHC2 (Vaisberg *et al.*, 1996), rat anti-D2LIC (Grissom *et al.*, 2002), rabbit anti-Polaris (Taulman *et al.*, 2001), mouse anti-β-tubulin (Sigma-Aldrich, St. Louis, MO), and a rabbit anti-p115 (Waters *et al.*, 1992). Secondary antibodies were obtained from Jackson Immunoresearch (West Grove, PA) and included donkey anti-rat rhodamine red X (712-295-153), donkey anti-mouse fluorescein isothiocyanate (715-095-150), and donkey anti-rabbit fluorescein isothiocyanate (711-096-152). Nuclei were stained with Hoechst 33528 (Sigma-Aldrich). Images were collected as described by Taulman *et al.* (2001).

RESULTS

Characterization of a Novel Dynein LIC Gene from Chlamydomonas

Studies of *cDHC1b* in *Chlamydomonas* have shown that this motor is required for flagellar assembly, but little is known about other components that might be associated with this Dhc (Pazour *et al.*, 1999; Porter *et al.*, 1999). We therefore analyzed the cDHC1b sequence to identify potentially conserved domains known to interact with specific subunits in other Dhc complexes. Conserved regions within the amino terminal one-third of cDHC1b include the two domains identified as the intermediate chain (IC) and LIC binding

sites in the rat cytoplasmic Dhc (DHC1a) (Tynan *et al.*, 2000a). These observations suggested that the *Chlamydomonas* cDHC1b might form a two-headed dynein complex that associates with related IC and LIC subunits. Indeed, recent work has identified a novel LIC, D2LIC, associated with the DHC2 complex in mammalian cells (Grissom *et al.*, 2002).

To determine whether a LIC similar to the mammalian D2LIC is present in *Chlamydomonas*, we screened the sequence databases and found an EST with limited sequence identity to the amino terminal region of the human D2LIC sequence. The sequence was recovered by RT-PCR and then used to screen cDNA and BAC genomic libraries and obtain full-length clones. Genomic Southern blot and RFLP analyses demonstrated that the *LIC* is a single copy gene that maps to linkage group IX, based on linkage to the molecular marker *NIT1* (see MATERIALS AND METHODS). Northern blot analysis revealed the presence of an ~2.3-kb transcript whose expression is up-regulated in response to deflagellation, as expected for a gene product involved in flagellar assembly or motility (Figure 1A). The estimated size of the transcript is similar to the size of the cDNA clone, consistent with the recovery of a full-length *LIC* gene.

The predicted amino acid sequence of the *Chlamydomonas* LIC is slightly longer than its mammalian counterparts (427 vs. 351 aa) and corresponds to a polypeptide with a predicted molecular mass of ~46.5 kDa (Figure 1B). This difference is due to the presence of alanine-rich region of ~60 aa located at the carboxy terminus of the *Chlamydomonas* LIC. However, sequence alignment programs reveal that the remainder of the LIC (aa 1–368) is closely related to the human D2LIC (Grissom *et al.*, 2002) and other D2LIC-like sequences identified in *Mus musculus*, *Drosophila melanogaster*, and *C. elegans* databases (22–28% identity, 43–47% similarity). Interestingly, no D2LIC-like sequences have been identified in yeast, fungi, or slime molds. The sequence conservation with the *C. elegans* sequence *F02D8.3* is particularly significant because this gene has recently been identified as a DAF-19–regulated X-box gene, *xbx-1*, whose expression is limited to sensory cilia. DAF-19 is an RFX-type transcription factor that regulates the expression of multiple genes involved in IFT, and disruption of *daf-19* results in the loss of cilia (Swoboda *et al.*, 2000).

Analyses of the LIC sequence for specific motifs identified parts of a P-loop sequence near the amino terminus (aa 47–54), a RAS signature motif (aa 46–105 and 216–235), and multiple potential phosphorylation sites (Figure 1C). The significance of the P-loop motif is unclear, because it is not conserved in the *C. elegans* XBX-1 LIC sequence (Schafer *et al.*, 2003), nor does it seem to be required for the function of the LICs associated with the conventional cytoplasmic dynein (Tynan *et al.*, 2000b; Yoder and Han, 2001). The RAS motif is conserved in other D2LIC sequences (Grissom *et al.*, 2002). A region near the carboxy terminus (aa 368–397) of the *Chlamydomonas* LIC is predicted to form an α-helical, coiled coil domain. Although the primary amino acid sequence is not conserved, a similar coiled coil seems to be present in the C-terminal region of the other D2LIC sequences. Comparison to the LICs associated with the conventional DHC1a also indicates limited sequence conservation with LIC1 and LIC2 (e.g., residues 46–300 share 20% identity and 39% similarity with residues 73–334 of rat LIC1). The conserved region includes domains identified as
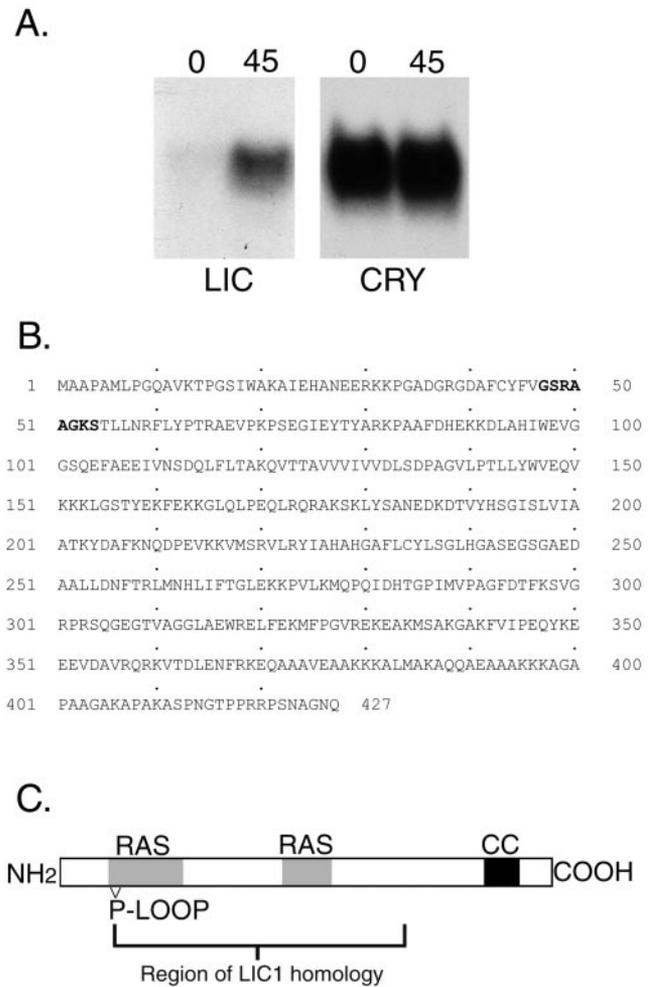
Figure 1. Identification of a novel LIC in *Chlamydomonas*. (A) Northern blot analysis. Total RNA isolated before (0) and 45 min after deflagellation (45) was size-fractionated on a gel, blotted to a nylon membrane, and hybridized overnight with a 367-base pair probe from the 5′ end of the *LIC* gene. Expression of the ~2.3-kb *LIC* mRNA was enhanced by deflagellation, compared with a control probe (*Cry1*) for a ribosomal protein subunit. (B) The predicted LIC amino acid sequence contains 427 residues and corresponds to an ~46.5-kDa polypeptide. The P-loop consensus motif is indicated in bold. (C). Schematic diagram of the LIC. Regions of homology with other dynein LICs include a P-loop motif near the amino terminus, a RAS signature motif, and a coiled coil domain near the carboxy terminus.

a potential cargo binding site (rat LIC1 residues 140–236, Tynan *et al.*, 2000b) and a Rab4a GTPase interaction site (human LIC1 residues 181–302; Bielli *et al.*, 2001) (Figure 1C).

LIC Cofractionates with cDHC1b Complex in *Chlamydomonas*

To study the cDHC1b complex in *Chlamydomonas*, we generated specific antibodies against both cDHC1b and LIC fusion proteins. Western blots of whole cell protein demonstrated that the affinity-purified cDHC1b antibody is isoform

specific; it recognizes a Dhc that is present in wild-type cells, but missing in *cDhc1b* null mutants (Figure 2A). cDHC1b is also found in preparations of isolated flagella (Figure 2B). Treatment with nonionic detergents releases ~50% of cDHC1b into the membrane + matrix fraction, and the rest is largely solubilized by extraction with increasing concentrations of MgATP (Figure 2B). The release of cDHC1b with detergent or ATP differs from that observed with axonemal Dhcs, which typically require high salt treatment to be efficiently extracted (Figure 2B).

Western blots of isolated flagella and related subfractions also show that the LIC is present in isolated flagella and released into the membrane + matrix and ATP extracts in a manner that qualitatively parallels the behavior of cDHC1b (Figure 2B). These results suggest that the LIC is a subunit of the cDHC1b complex, and not a component of another dynein complex present in the flagellum. To further demonstrate that the LIC is specifically associated with cDHC1b, we performed a series of immunoprecipitation reactions by using the LIC antibody and then analyzed the immunoprecipitates on Western blots probed with the cDHC1b antibody. As shown in Figure 2C, the affinity-purified LIC antibody coimmunoprecipitated cDHC1b, whereas control reactions with other affinity-purified antibodies did not. Interestingly, although the conserved dynein light chain, LC8, is present in the dynein extracts, we did not detect a significant enrichment of LC8 in the LIC immunoprecipitates (Figure 2C).

Sucrose gradient centrifugation of DHC2 complexes isolated from mammalian tissue culture cells or rat testes has shown that this complex typically sediments at ~15S (Vaisberg *et al.*, 1996; Criswell and Asai, 1998; Grissom *et al.*, 2002). Because extracts of *Chlamydomonas* flagella contain several axonemal dyneins, we isolated the cDHC1b complex from either *pf28* strains (lacking the outer arm dyneins) or E8 strains (lacking outer arm dyneins and the I1 inner arm dynein) by using various extraction conditions. The extracts were fractionated either by sucrose density centrifugation or ion exchange FPLC, and the resulting fractions were then analyzed on Western blots probed with the cDhc1b antibody. Extraction with high salt followed by sucrose density gradient centrifugation yielded cDHC1b complexes sedimenting at ~12S (Figure 3A). However, cDHC1b complexes prepared either by detergent extraction or ATP extraction alone sedimented at ~19S (Figure 3B). Shifts in the sedimentation behavior of dynein complexes after exposure to high salt have been observed with other dynein isoforms and typically reflect dissociation of loosely bound subunits (Goodenough and Heuser, 1984; King *et al.*, 2002). The sedimentation behavior shown in Figure 3 suggests that the cDHC1b complex is also a two-headed dynein complex that becomes dissociated in the presence of high salt.

To determine whether LIC copurifies with cDHC1b after the different extraction protocols, Western blots of the gradient fractions were probed with the LIC antibody. As shown in Figure 3A, the majority of LIC peaked with cDHC1b at ~12S in the high salt extracts, although a small amount can also been seen near the top of the gradient, at ~6S. Similar results were observed with the mammalian D2LIC (Grissom *et al.* 2002). However, after detergent or ATP extraction, the majority of the *Chlamydomonas* LIC
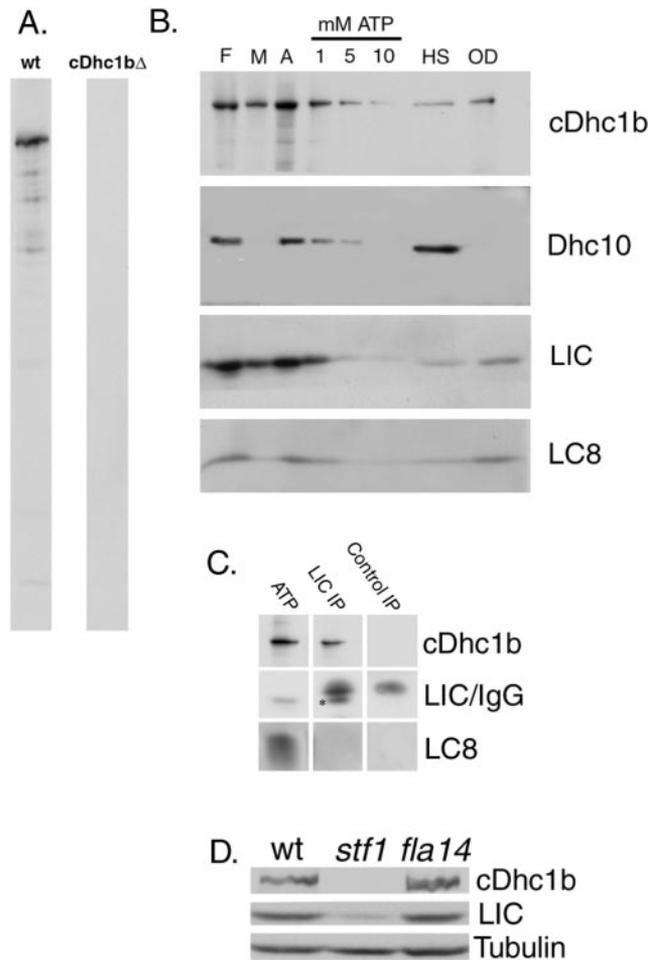
Figure 2. Association of the LIC with cDHC1b in flagellar extracts. (A) Whole cell extracts were made from wild-type and *cDhc1b* mutant cells and probed with an affinity purified cDHC1b antibody to demonstrate the specificity of the cDHC1b antibody. (B) Isolated flagella (F) from the outer arm mutant *pf28* were first treated with a nonionic detergent to separate the soluble membrane plus matrix fraction (M) from isolated axonemes (A). Axonemes were then sequentially extracted with increasing concentrations of MgATP (1, 5, and 10 mM), followed by 0.6 M NaCl (HS). The outer doublets (OD) represent the axonemal proteins remaining after extraction. Gels were loaded stoichiometrically, blotted to polyvinylidene difluoride, and probed with the antibodies indicated. The LIC coextracts with cDHC1b. (C) Isolated axonemes prepared from an E8 strain lacking both outer arm and I1 inner arm dyneins were extracted with 10 mM MgATP. The ATP extract was then incubated with protein A-Sepharose beads containing either the affinity-purified LIC antibody or a control IgG. The ATP extract (lane 1) and the immunoprecipitates (lanes 2 and 3) were analyzed on Western blots probed with antibodies to cDHC1b, LIC, and LC8. Because the LIC is ~46.5-kDa (see *), it is difficult to resolve from the IgG heavy chain and quantitate the extent of LIC immunoprecipitation. However, it is clear that the LIC antibody coimmunoprecipitates cDhc1b, whereas the control antibody does not. LC8, shown here on a 5–20% gradient gel, is present in the ATP extract, but not enriched in the LIC immunoprecipitate. (D) Western blots of equivalent numbers of wild-type, *cDhc1b* null (*stf1-1*), and *LC8* null (*fla14*) cells were probed with antibodies to cDhc1b, LIC, and tubulin.

A.

B.
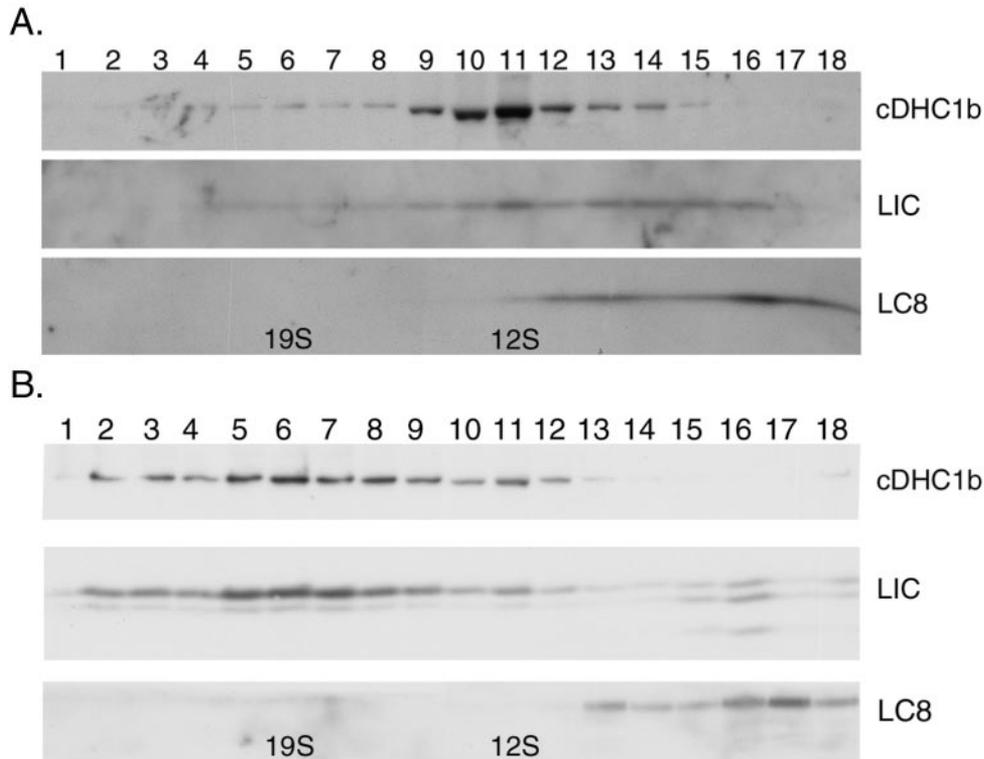
Figure 3. Copurification of the LIC with cDHC1b on sucrose density gradients. (A) A high salt extract of E8 axonemes (lacking the outer arm and I1 inner arm dyneins) was analyzed on a 5–20% sucrose density gradient. The resulting fractions were separated on a 5–15% PAGE, blotted to polyvinylidene difluoride, and probed with the antibodies indicated. (B) A similar Western blot containing sucrose gradient fractions from a 10 mM MgATP extract of E8 axonemes. The peak of cDHC1b and LIC has shifted to ~19S.

cosediments with cDHC1b at ~19S (Figure 3B). The close association of the LIC with cDHC1b throughout different purification procedures is consistent with the hypothesis that they are subunits of the same motor complex.

The highly conserved dynein light chain, LC8, is a common subunit of all homo- or heterodimeric dynein complexes, including the conventional cytoplasmic dynein, the outer dynein arms, and the I1 inner arm dynein (King *et al.*, 1996; Harrison *et al.*, 1998). In addition, LC8 null mutants are defective in flagellar assembly and retrograde IFT (Pazour *et al.*, 1998). These results suggested that LC8 might also be a subunit of the retrograde motor. We therefore analyzed Western blots of dynein extracts fractionated either by sucrose density gradient centrifugation or FPLC to determine whether LC8 copurifies with the cDHC1b complex. These extracts were prepared from either *pf28* or E8 flagella to avoid contamination by LC8 cosedimenting with the outer arm dyneins or the I1 inner arm complex. As shown in Figure 3, LC8 is present in E8 extracts, but the majority of LC8 does not cosediment with the cDHC1b/LIC complex when prepared by either by ATP or high salt extraction followed by sucrose gradient centrifugation. As mentioned above, LC8 was also not observed on Western blots of LIC immunoprecipitates (Figure 2C). However, LC8 does copurify with the I1 dynein in *pf28* extracts, when analyzed either by sucrose density centrifugation or FPLC (Harrison *et al.*, 1998; our unpublished data). If LC8 is a subunit of the cDHC1b/LIC complex then its association with this complex seems to be weaker than its association with the I1 dynein.

LIC Colocalizes with cDHC1b Complex in Wild-Type and Flagellar Mutants

The cellular distribution of both cDHC1b and the LIC was examined by immunofluorescence microscopy by using the affinity-purified antibodies described above (Figure 4). In wild-type cells, the cDHC1b antibody primarily stained the anterior portion of the cell, in the region around the basal bodies. Bright, punctate staining was also visible along the length of the two flagella (Figure 4, A and B). Staining wild-type cells with the LIC antibody produced a pattern virtually identical to that seen with the cDHC1b antibody (Figure 4, C and D). The LIC was predominantly localized to the peribasal body region and in punctate spots along the length of the two flagella. Significantly, however, the LIC seems to be completely mislocalized in the *cDhc1b* mutant, *stf1* (Figure 4, G and H). There was no staining of the flagellar stumps, and the peribasal body staining was also absent. Some LIC staining could be seen in the cell body, primarily in punctate spots that could not be correlated with any specific organelle, but the total signal seemed to be weaker than in wild-type cells. Western blots of wild-type and *stf1* cells probed with the LIC antibody confirmed that LIC protein levels are reduced in the *cDhc1b* mutant background (Figure 3D). Interestingly, it is known that a significant portion of the *cDHC1b* gene is deleted in the *stf1-1* mutant, including the region predicted to encode the LIC binding site (Porter *et al.*, 1999). Therefore, these results indicate that proper localization of the LIC requires the presence of the cDHC1b motor and further suggest that the LIC may be destabilized in the absence of the heavy chain,
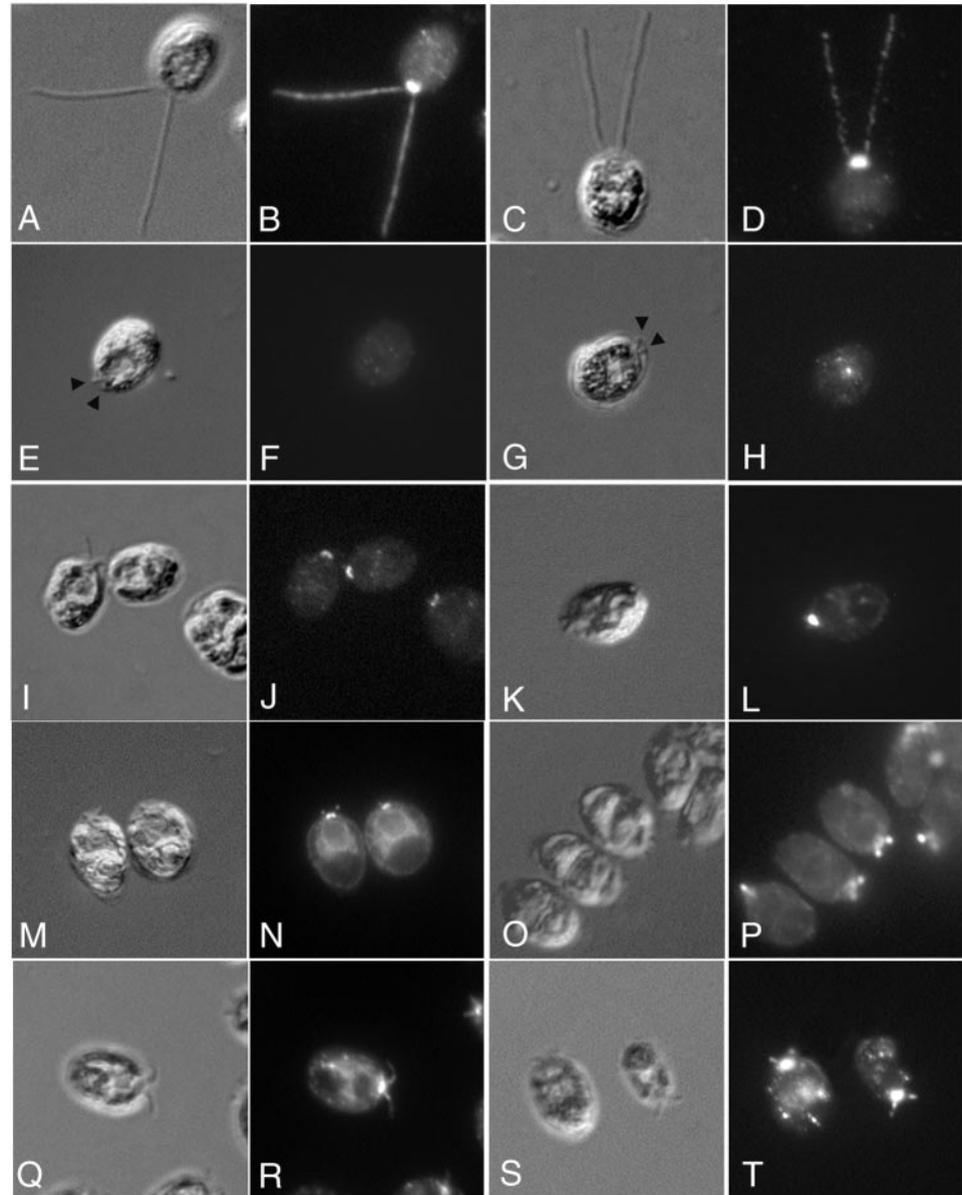
Figure 4. Colocalization of the LIC with cDHC1b in wild-type and dynein mutant cells. In the top row, fixed wild-type cells were stained with antibodies to cDHC1b (A and B) or LIC (C and D) and imaged by differential interference contrast (DIC) microscopy (A and C) or epifluorescence (B and D). In the second row, *cDhc1b* mutant cells (*stf1*) were stained with antibodies to cDHC1b (E and F) or LIC (G and H). Arrowheads indicate the position of the flagellar stubs in DIC images (E and G). Note the absence of cDHC1b staining. LIC staining is also dispersed and reduced in *cDhc1b* mutant cells. In the third row, *LC8* mutant cells (*fla14*) were stained with antibodies to cDHC1b (I and J) or LIC (K and L). Note that both cDHC1b and LIC accumulate in peribasal body region, but not in the flagellar stubs. In the fourth row, *cDhc1b* mutant cells were stained with antibodies to FLA10 kinesin (M and N) or the p172 subunit of IFT complex B (O and P). In the bottom row, *LC8* mutant cells were stained with antibodies to the FLA10 kinesin subunit (Q and R) or p172 (S and T). Note the accumulation of both components in the short flagella of *stf1* and *fla14*.

consistent with the observation that they are subunits of the same complex.

The altered localization of the LIC in the *stf1* mutant is also distinct from the mislocalization observed with other IFT components. For example, both the FLA10 kinesin and the IFT particles are found primarily in the peribasal body region in wild-type cells (Cole *et al.*, 1998). They become concentrated in the short flagellar stumps in the *stf1* mutant via anterograde IFT, but fail to be recycled to the cell body in the absence of retrograde IFT (Figure 4, M–P; Pazour *et al.*, 1999; Porter *et al.*, 1999). The FLA10 motor and IFT particles are therefore transported to the peribasal body region and into the flagellum in the absence of cDHC1b motor activity, but the LIC is not. The association of the LIC with cDHC1b

is therefore fundamentally different from that of the cDHC1b motor with its proposed cargoes.

Because LC8 has been proposed to be a subunit of the cDHC1b complex, we also analyzed the distribution of cDHC1b and the LIC in the *LC8* mutant *fla14* (Figure 4, I–L). *fla14* mutant cells are defective in retrograde IFT and assemble short flagella filled with IFT subunits (Pazour *et al.*, 1998). Interestingly however, Western blots of whole *fla14* cells probed with cDHC1b and LIC antibodies indicate that both polypeptides are present at wild-type levels (Figure 3D). In addition, indirect immunofluorescence of *fla14* cells indicates proper localization of both cDHC1b (Figure 4, I and J) and the LIC (Figure 4, K and L) in the peribasal body region, but we were unable to detect significant levels of either
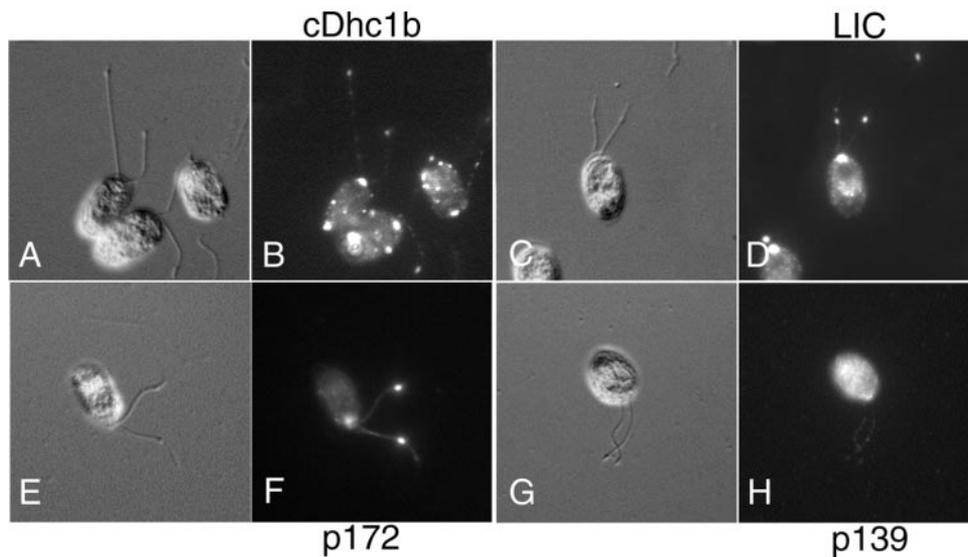
Figure 5. Colocalization of the LIC with cDHC1b in a retrograde IFT mutant. *fla15* cells have defects in raft complex A and retrograde IFT (Piperno *et al.*, 1998). At the permissive temperature, these mutants develop one to two small blebs along the length of their flagella that can be detected by differential interference contrast microscopy (A, C, E, and G). The *fla15* cells were stained with antibodies to cDHC1b (A and B), the LIC (C and D), the p172 subunit of IFT complex B (E and F), and the p139 subunit of IFT complex A (G and H). Note that the blebs do not stain with the p139 antibody, but they do stain with the cDHC1b, LIC, and p172 antibodies.

cDHC1b or LIC within the short flagellar stubs. These results suggest that the cDHC1b/LIC complex is intact and appropriately targeted to the minus ends of the microtubules in the anterior region of the cell. LC8 does not seem to be required for the formation of the cDHC1b/LIC complex or its targeting to the peribasal body region. However, LC8 does seem to be required for the efficient targeting or transport of the cDHC1b motor into the flagellar compartment (see DISCUSSION).

Temperature-sensitive mutations that alter the stability of raft complex A components (*fla15*, *fla16*, and *fla17*) also disrupt retrograde IFT and flagellar assembly (Piperno *et al.*, 1998). The mutants seem to be defective in the remodeling of IFT particles that normally occurs at the distal tips of the flagella (Iomini *et al.*, 2001). These strains accumulate IFT motors and raft complex B components, but not raft complex A components, in small blebs located between the axoneme and the flagellar membrane (Iomini *et al.*, 2001; Figure 5, E–H). To verify that the LIC colocalizes with cDHC1b under these conditions, we analyzed the distribution of the LIC in the collection of retrograde IFT mutants. As shown in Figure 5 (C and D), staining *fla15* cells with the LIC antibody clearly demonstrated the concentration of the LIC in flagellar bulges. The pattern is identical to that observed with the cDHC1b antibody, strong peribasal body staining, punctate staining along length of the flagella, and an accumulation in the blebs (Figure 5, A and B; Iomini *et al.*, 2001). Identical results were also observed with two other retrograde IFT mutants, *fla16* and *fla17*. The colocalization of the LIC with cDHC1b in the flagellar bulges is consistent with the hypothesis that this subunit might mediate or regulate the attachment of the cDHC1b motor to the IFT particles.

The cDHC1b/LIC Complex Becomes Concentrated in the Flagellar Tips in Length Control Mutants

Little is known about the specific signals that control flagellar assembly and/or mediate the switch between anterograde and retrograde IFT in the flagellum, but several stud-

ies have suggested that this process is altered in a group of length control mutants that assemble abnormally long flagella (Asleson and Lefebvre, 1998; Barsel *et al.*, 1988). For instance, microtubule turnover at the plus end of the flagellum seems to be decreased in *lf2* cells (Marshall and Rosenbaum, 2001). Moreover, other work suggests that regulation of flagellar assembly and IFT may depend in part on structures located at the flagellar tips (Tuxhorn *et al.*, 1998; Iomini *et al.*, 2001). We therefore stained a collection of *long flagella* (*lf*) mutants with antibodies to several IFT polypeptides to determine whether the distribution of IFT components might be altered in the length control mutants. As shown in Figure 6, staining of *lf1* cells with antibodies to cDHC1b (Figure 6, A and B) or LIC (Figure 6, C and D) reveals a typical wild-type pattern, with the exception that both polypeptides are also concentrated in blebs located at the flagellar tips. The flagellar tip staining is consistent throughout the population of *lf1* cells, and it is never observed in healthy cultures of wild-type cells. In addition, IFT complex A subunit p139 (Figure 6, G and H), IFT complex B subunit p172 (Figure 6, E and F), and the FLA10 motor (Figure 6, I and J) all become concentrated at the flagellar tips of the *lf1* cells. Flagellar tip staining was also observed in other long flagella mutants, although not as consistently as in *lf1* (Figure 6, K and L). As wild-type cells maintain a constant pool of IFT components irrespective of flagellar length (Marshall and Rosenbaum, 2001), the accumulation of IFT components at the tips of the long flagella suggests that the cDHC1b motor and retrograde transport are not properly regulated in the length control mutants (see DISCUSSION).

D2LIC Colocalizes with DHC2 at Sites of Axoneme Assembly in Mammalian Cells

Immunofluorescence studies in tissue culture cells have shown that the DHC2/D2LIC complex is concentrated in the centrosomal region and closely associated with the Golgi apparatus (Vaisberg *et al.*, 1996; Grissom *et al.*, 2002). However, studies in *Chlamydomonas* and *C. elegans* have indicated
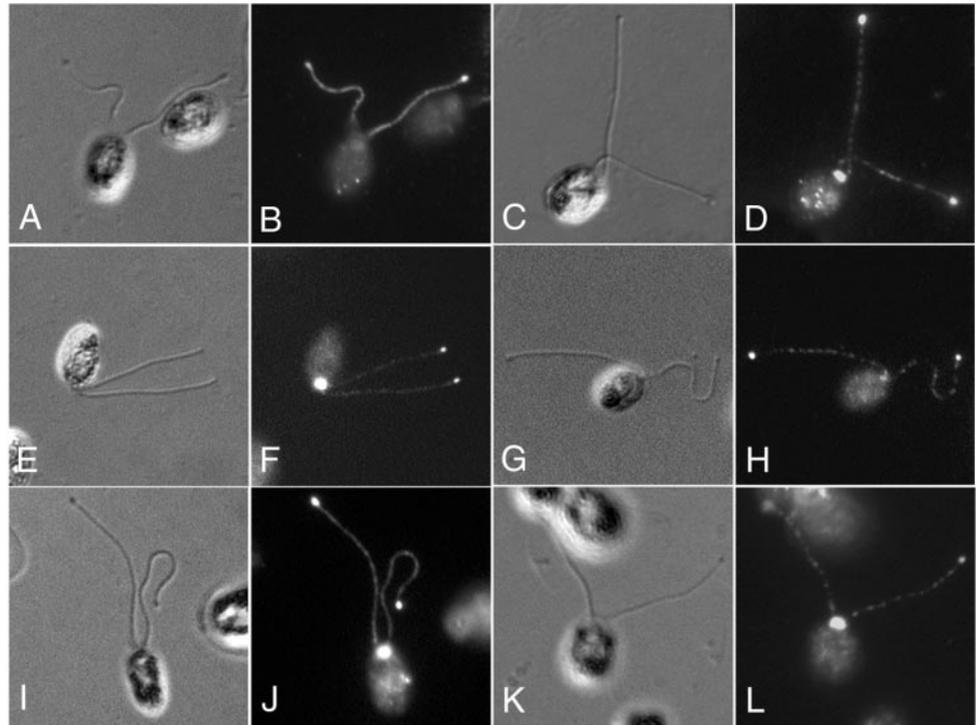
Figure 6. Redistribution of IFT motors and IFT particles in a length control mutant. *lf1* cells assemble flagella that are 2 to 3 times wild-type length (Barsel *et al.,* 1988; Aselson *et al.,* 1998). Small bulges are often visible at the tips of the *lf1* flagella by differential interference contrast microscopy. *lf1* cells were stained with antibodies to cDHC1b (A and B), LIC (C and D), p172, (E and F), p139 (G and H), and the FLA10 kinesin (I and J). Note the accumulation of all components at the flagellar tips (cDHC1b staining of the peribasal body region is out of the plane of focus in B). (K and L) Staining of *lf3* cells with antibodies to the LIC.

the primary function of the cDHC1b isoform is its role in flagellar assembly (Pazour *et al.,* 1999; Porter *et al.,* 1999; Wicks *et al.,* 2000). Because the centrosomal region is also the site of assembly of the primary cilium (Wheatley *et al.,* 1996; Poole *et al.,* 1997, 2001), we reexamined the distribution of the complex in mammalian cells relative to sites of cilia assembly. Preliminary experiments with polarized cultures of MDCK cells indicated that D2LIC is present in a diffuse pattern throughout the apical cytoplasm (Figure 7, A and D). However, when cells are viewed at a higher focal plane, D2LIC is clearly enriched at the base of and within the primary cilia (Figure 7, A–D). The D2LIC staining is similar to that reported for the IFT particle subunit, Polaris (Taulman *et al.,* 2001). Moreover, we did not detect significant colocalization of D2LIC with the Golgi apparatus in the MDCK cells (Figure 7, D–F). These observations prompted us to analyze the distribution of DHC2 and D2LIC in situ in mouse tissues.

Immunofluorescence analysis with DHC2 and D2LIC antibodies revealed that both polypeptides are prominent components in ciliated cells of the lung (Figure 8), efferent duct (Figure 9), and brain (our unpublished data). Anti-D2LIC (Figure 8, A, D, and G) staining in the lung is clearly restricted to a small number of cells lining the respiratory airways, and a similar pattern is observed with the antibody to DHC2 (Figure 8F). Double staining with a tubulin antibody (Figure 8, B and C) reveals that the DHC2- and D2LIC-positive cells are the ciliated cells of the bronchioles. Double staining with the Polaris antibody further demonstrates that D2LIC colocalizes with mammalian IFT particles in both the apical cytoplasm and the cilia (Figure 8, G–I). Higher magnification views of the ciliated cells show that both DHC2 and D2LIC are present along the length of the axonemes

(Figure 8, insets). The axoneme staining shown herein differs from a previous report, in which DHC2 was only found in the apical cytoplasm of isolated tracheal cells (Criswell *et al.,* 1996).

To verify that the localization of DHC2 and D2LIC in the ciliary axoneme is a general feature of mammalian tissues, we also examined the distribution of the two proteins in the highly polarized epithelium of the efferent duct. The efferent duct transports material from the rete testis to the epididymis and contains extensive motile cilia that are easily viewed in tissue sections. D2LIC staining is again restricted to the ciliated cells of the efferent duct, and D2LIC seems to be concentrated in the apical cytoplasm at the base of the cilia (Figure 9, A–C). However, when individual cells are examined at higher magnification (Figure 9, D, G, and J), D2LIC can be also be detected within the ciliary axoneme, where it overlaps with both DHC2 (Figure 9, H and I) and the IFT particle protein Polaris (Figure 9, K and L).

To compare the localization of the DHC2/D2LIC complex with that of the Golgi apparatus, we costained sections of the efferent duct with an antibody to the Golgi marker p115. As shown in Figure 10, the apical distribution of the D2LIC is clearly distinct from the position of the Golgi apparatus within the cells of the duct. In addition, it is possible to see connective tissue cells outside the duct that are stained with the Golgi antibody, but unstained with the D2LIC antibody (Figure 10, A–C). When duct cells are viewed at higher magnification (Figure 10, D–F), the D2LIC staining is concentrated in the apical cytoplasm, at the base and along the length of the ciliary axonemes. Although both D2LIC and the Golgi apparatus are found in the apical region, D2LIC does not seem to be enriched at the site of the Golgi apparatus in these highly polarized cells (Figure 10).
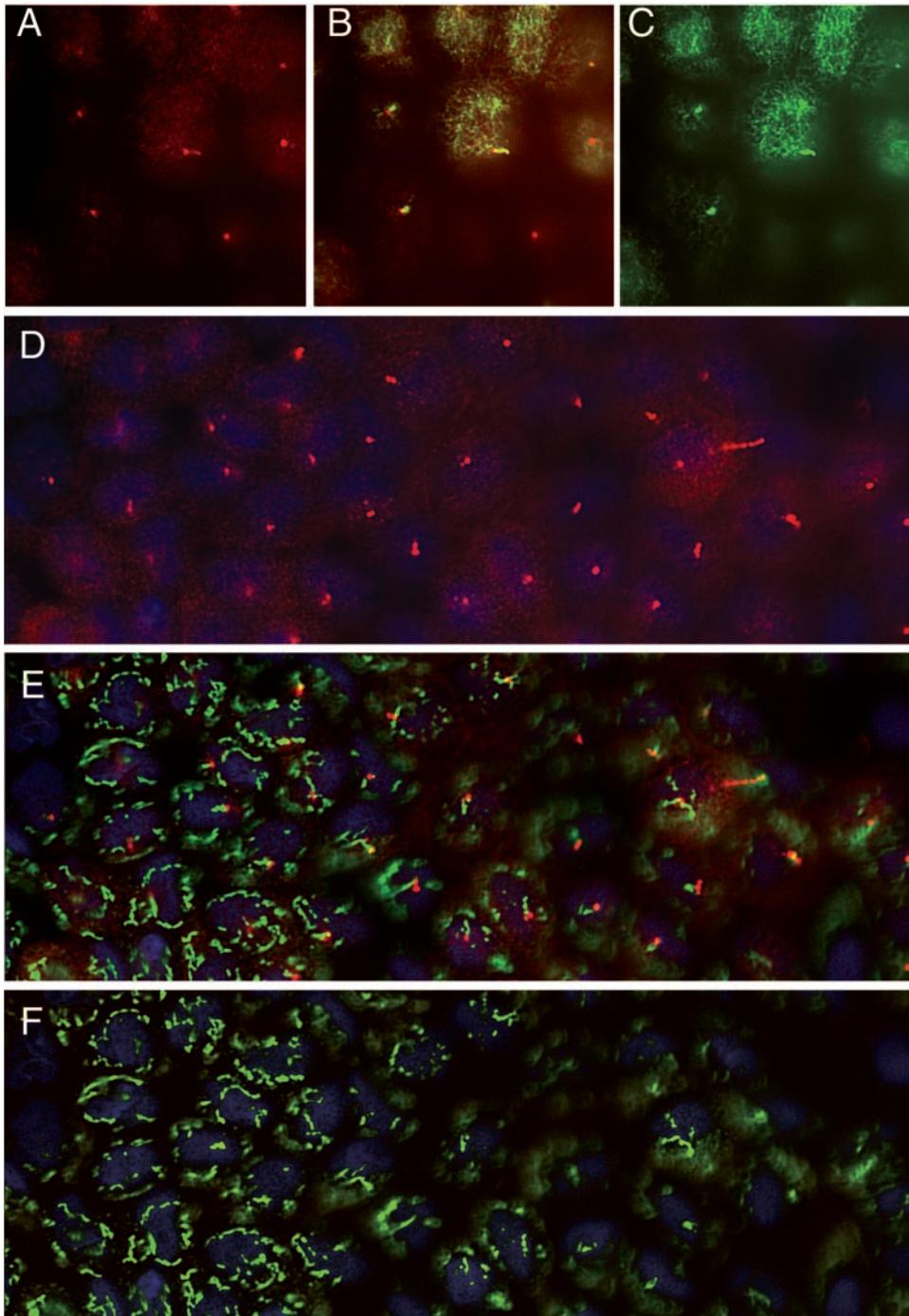
Figure 7. D2LIC colocalizes with primary cilia in MDCK cells. Confluent cultures of polarized MDCK cells were stained with antibodies to D2LIC (shown in red) and either tubulin or the Golgi marker p115 (shown in green). The cells shown in A–C were costained with anti-D2LIC and anti-tubulin and then viewed from above, at the level of the apical cytoplasm and primary cilia. D2LIC staining (A), merged image (B), and tubulin staining (C). The cells shown in D–F were costained with anti-D2LIC, anti-p115, and Hoescht. D2LIC staining (D), merged image (E), and p115 staining (F). The Golgi apparatus is often out of focus in optimal views of the primary cilia. D2LIC is abundant in the apical cytoplasm, but clearly enriched in the primary cilia.

DISCUSSION

A Novel Dynein Light IC Associated with the Retrograde Motor for IFT

In this study, we have identified the *Chlamydomonas* homolog of the mammalian D2LIC (Figure 1), and we have shown that this novel LIC is a tightly bound subunit of the cDHC1b complex. The specific immunoprecipitation of cDHC1b with the LIC (Figure 2), their cosedimentation on sucrose density gradients (Figure 3), and their consistent colocalization in both wild-type cells and a collection of retrograde IFT mutants (Figures 4 and 5) all demonstrate that these two polypeptides are subunits of the same motor complex. By analogy to the LICs associated with the conventional cytoplasmic dynein (Dell *et al.*, 2000; Tynan *et al.*, 2000b; Yoder and Han, 2001), it seems likely that the LIC
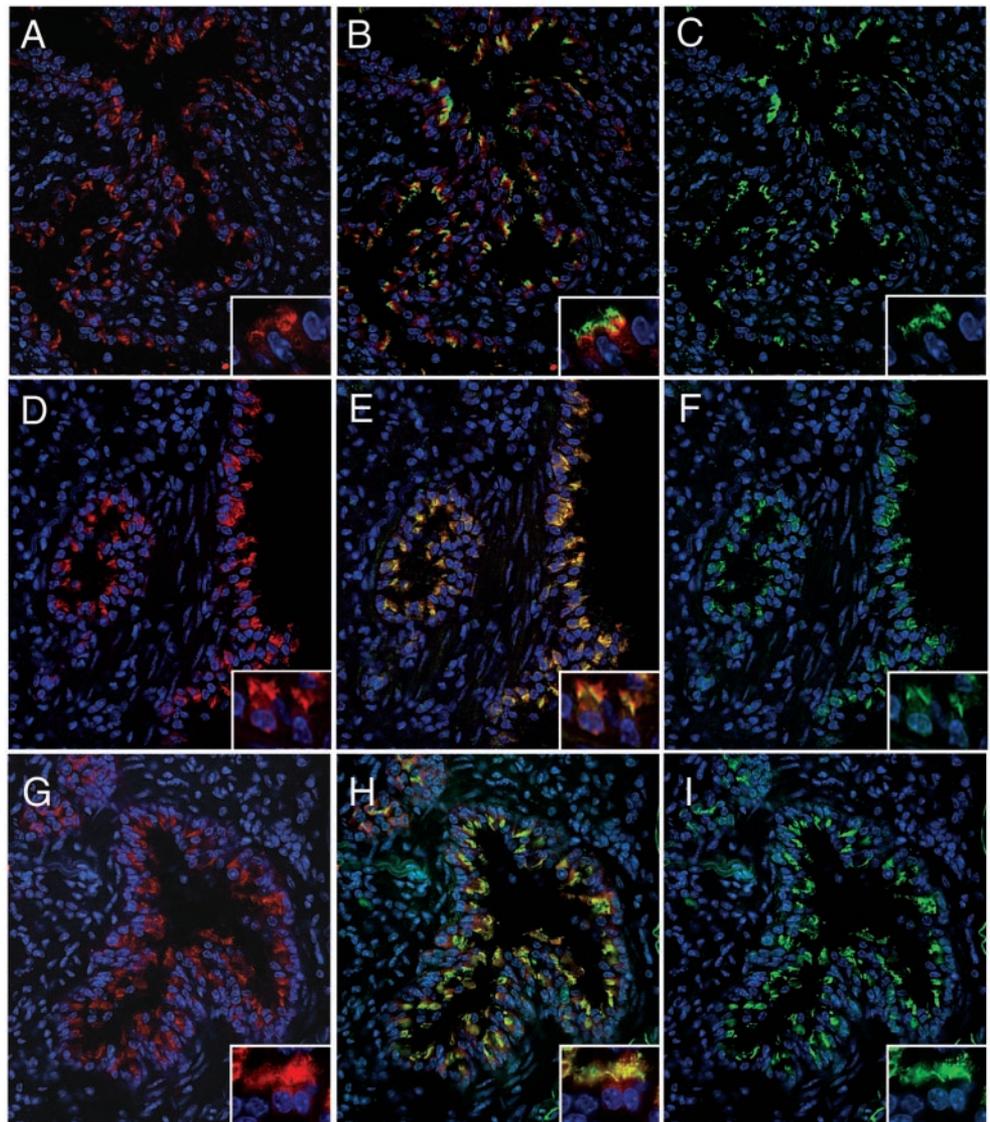
Figure 8. The mammalian D2LIC colocalizes with DHC2 and the IFT particle subunit Polaris in the ciliated epithelium of the lung. Isolated mouse lungs were fixed, sectioned, and stained with an affinity-purified rat antibody to the mammalian D2LIC (shown in red on the left; A, D, and G). The sections were costained with a mouse monoclonal antibody to tubulin (C), or affinity-purified rabbit antibodies to DHC2 (F), or Polaris (I), all shown in green on the right. Merged images are shown in the middle (B, E, and H). Nuclei were stained with Hoechst and are shown in blue. The inset in each panel shows two to three cells at a higher magnification. Note that staining is restricted to ciliated cells and seems to be concentrated in the apical cytoplasm and the ciliary axonemes.

associated with cDHC1b/DHC2 plays an essential role in mediating the attachment of the motor to its cargo(s) and/or regulating its activity. As previous work has shown that cDHC1b is required for both flagellar assembly and retrograde IFT (Pazour *et al.*, 1999; Porter *et al.*, 1999; Signor *et al.*, 1999; Wicks *et al.*, 2000), it also seems likely that the LIC is essential for retrograde IFT in all ciliated cells. Indeed, mutant analysis in *C. elegans* has now shown that the *xbx-1* gene encodes the homologous LIC and that this LIC is required for retrograde IFT and ciliary assembly in sensory neurons of the worm (Schafer *et al.*, 2003). A conserved role in retrograde IFT is also consistent with the observation that no D2LIC homologs have been identified in nonciliated organisms.

The association of the LIC with cDHC1b seems to be stronger than the association of either component with the dynein light chain LC8. LC8 is thought to be a universal subunit of homodimeric or heterodimeric dynein complexes

(King *et al.*, 1996). In addition, *LC8* mutants in *Chlamydomonas* are specifically defective in flagellar assembly and retrograde IFT (Pazour *et al.*, 1998). We therefore expected LC8 to copurify with cDHC1b and the LIC, but thus far we have not detected a significant enrichment of LC8 in the complex (Figures 2C and 3). However, recent studies on the subunit composition of the conventional cytoplasmic dynein have shown that the IC/LC complex can be more readily dissociated from DHC1a than the LICs (King *et al.*, 2002), and so it is possible that LC8 was released from the cDHC1b/LIC complex during our purification procedures. In addition, our immunofluorescence studies revealed that the cDHC1b/LIC complex is not concentrated in the flagellar stumps of the *fla14* mutant, unlike other IFT components such as the FLA10 kinesin or IFT particles (Figure 4). LC8 therefore plays a critical but poorly understood role in regulating the targeting and/or transport of the cDHC1b motor into the flagella. Further work is needed to identify and characterize
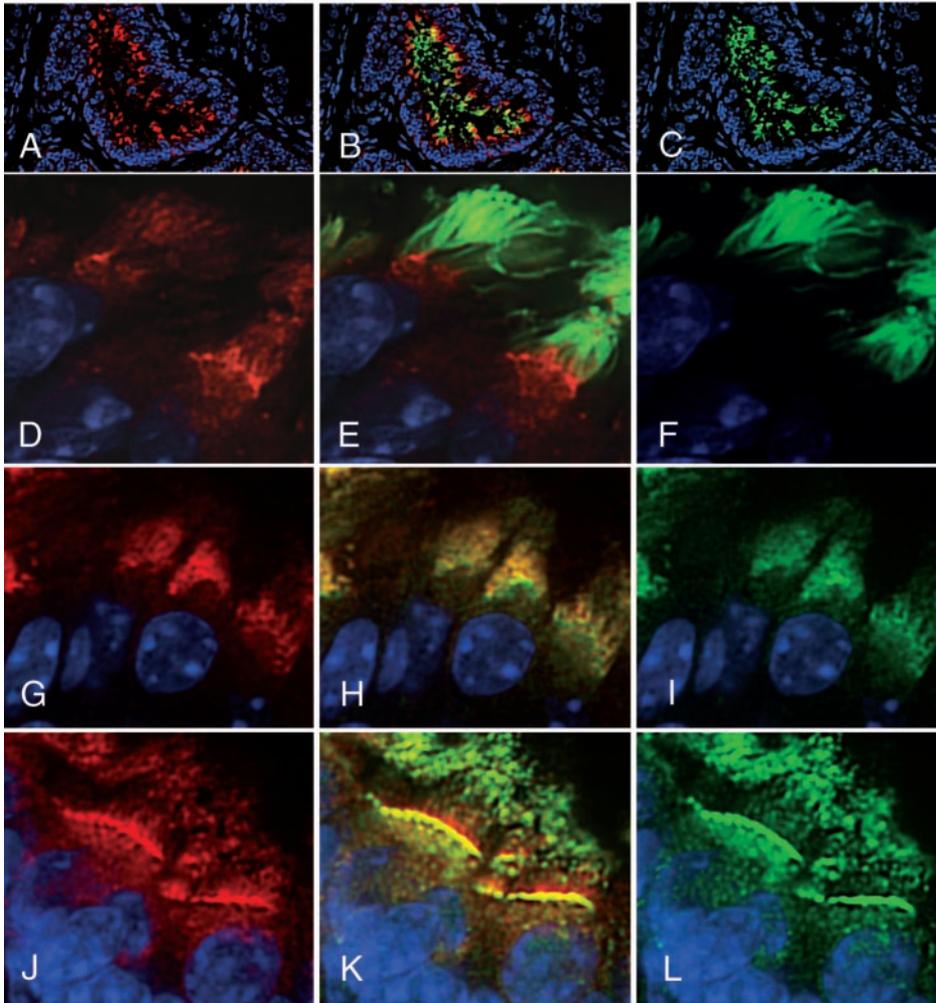
Figure 9. D2LIC colocalizes with DHC2 and the IFT particle subunit Polaris in the ciliated epithelium of the efferent duct. Isolated mouse efferent ducts were fixed, sectioned, and stained with an affinity-purified rat antibody to the mammalian D2LIC (shown in red on the left in A, D, G, and J). The sections were costained with antibodies to tubulin (C and F), DHC2 (I), or Polaris (L), all shown in green on the right. Merged images are shown in the middle (B, E, H, and K). (A–C) Low-magnification views displaying cross sections through an efferent duct; the remaining panels are higher magnification views of the ciliated cells of the ducts.

other subunits of the cDHC1b motor complex and to determine how these subunits might interact with LC8. One possibility is that LC8 is required for the loading of the cDHC1b/LIC complex (and other axonemal complexes) onto the anterograde transport machinery, either by promoting their stability, or facilitating their selective recognition by docking structures located near the basal body region (Deane *et al.*, 2001). An alternative hypothesis is that LC8 might be a subunit of another complex that also contributes to IFT.

Localization of D2LIC and DHC2 in Mammalian Cells

Our immunofluorescence studies of isolated mouse tissue demonstrate that the DHC2/D2LIC complex is most abundant in highly ciliated cells, where it localizes to the apical cytoplasm and the ciliary axonemes in both the lung and efferent duct (Figures 8–10). A similar pattern was evident in the brain, where anti-D2LIC staining was restricted to the ciliated ependymal cells lining the ventricles (our unpublished data). The DHC2/D2LIC complex also seems to be

more closely associated with the mammalian IFT particle protein Polaris (Figures 8 and 9) than with the Golgi apparatus in these ciliated cells (Figure 10). The apical cytoplasm of ciliated epithelial cells is comparable with the peribasal body region in *Chlamydomonas*, and so the distribution of the DHC2/D2LIC complex is essentially identical to that of cDHC1b/LIC complex in *Chlamydomonas*. These observations suggest that the DHC2/D2LIC complex functions as the retrograde motor for IFT in ciliated epithelia.

The DHC2/D2LIC complex is probably also required for the assembly of nonmotile, primary cilia in mammalian cells. Primary cilia are present in most cultured cells, but a single cilium is often difficult to observe without specific antibodies (Wheatley *et al.*, 1994, 1996). The assembly of primary cilia can also vary with culture conditions and the stage of the cell cycle (Tucker *et al.*, 1979; Alieva *et al.*, 1999). However, when the primary cilium is analyzed directly, this organelle colocalizes with the centrosome, and it is often in proximity to the Golgi apparatus (Poole *et al.*, 1997, 2001; Aughsteen, 2001). Previous studies have shown that the DHC2/D2LIC complex localizes to the centrosomal region in mammalian tissue culture cells, where it overlaps with the
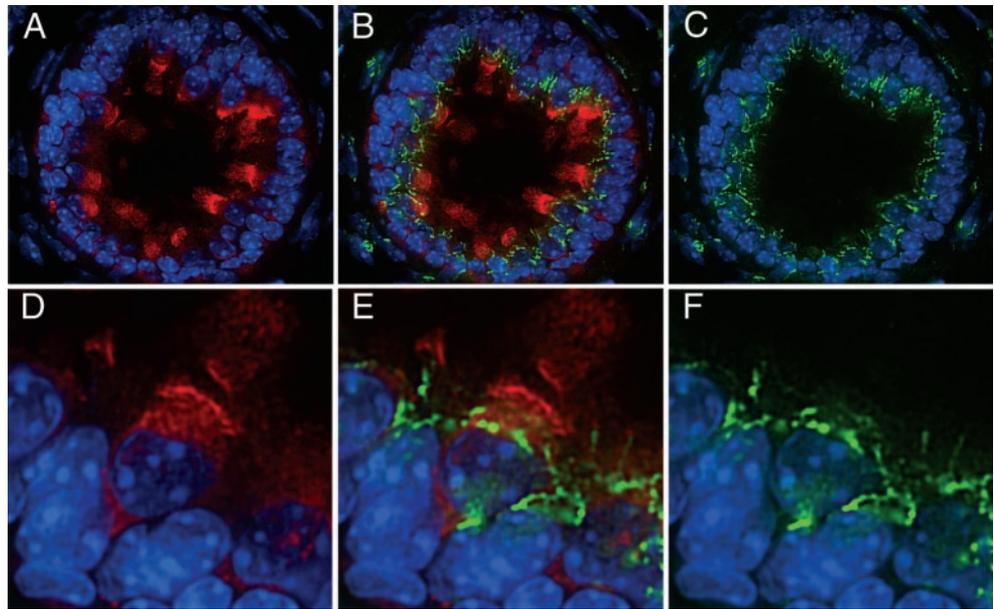
Figure 10. D2LIC does not colocalize with the Golgi apparatus in the efferent duct. Sections of efferent ducts were stained with the affinity-purified rat antibody to D2LIC (shown in red in A and D) and a rabbit antibody to the Golgi marker p115 (shown in green in C and F). Merged images are shown in B and E. (A–C) Low-magnification views of a single efferent duct and surrounding connective tissue. (D–F) higher magnification views of individual duct cells.

position of the Golgi apparatus (Vaisberg *et al.*, 1996; Grissom *et al.*, 2002). If the DHC2/D2LIC complex is required for the assembly of the primary cilium, its apparent colocalization with the Golgi apparatus may be related to their mutual association with the centrosome. Indeed, a significant fraction of the D2LIC does remain associated with the centrosomal region after treatment of cells with brefeldin A to disrupt the Golgi apparatus (see Figure 7 in Grissom *et al.*, 2002). Moreover, when we stained cultures of highly polarized MDCK cells, we observed that the DHC2/D2LIC complex is not only present in the apical cytoplasm but also it is clearly enriched at the base and along the length of the primary cilium in each cell (Figure 7). The phenotypes of the *cDhc1b* (*che-3*) and the *LIC* (*xbx-1*) mutants in *C. elegans* show that the cDHC1b/LIC complex is required for the assembly of nonmotile sensory cilia in the worm (Wicks *et al.*, 2000; Schafer *et al.*, 2003). In the mouse, knockouts of kinesin II subunits have demonstrated that the anterograde IFT motor is essential for ciliary assembly in mammalian tissues (Nonaka *et al.*, 1998; Marszalek *et al.*, 1999). The generation of mouse mutants that lack a functional DHC2 or D2LIC subunit may likewise reveal a similar role for the retrograde motor in mammalian cells.

Regulation of the cDHC1b/LIC Complex

The phenotypes of *cDhc1b* mutants in both *Chlamydomonas* and *C. elegans* indicate that the primary function of cDHC1b is its role as the retrograde motor for IFT (Pazour *et al.*, 1999; Porter *et al.*, 1999; Signor *et al.*, 1999; Wicks *et al.*, 2000). However, in wild-type cells, most of the cDHC1b/LIC complex is found at the peribasal body region. Thus, there must be at least two sites where the activity of the cDHC1b complex is regulated. First, the cDHC1b motor must be brought into the flagellum in an inactive form. After reaching the plus ends of the microtubules at the flagellar tips, the cDHC1b motor must be then activated for retrograde IFT to the cell body.

Studies on other dynein isoforms have shown that controlled phosphorylation and dephosphorylation of IC and LIC subunits is one mechanism for regulating dynein activity, either by switching motor activity on and off (Habermacher and Sale, 1997; Yang and Sale, 2000), or by regulating the interaction of the motor with potential cargoes (Vaughan *et al.*, 2001). For example, the LIC subunits associated with the conventional cytoplasmic dynein can be phosphorylated at multiple sites (Gill *et al.*, 1994; Hughes *et al.*, 1995; Dell *et al.*, 2000; Addinall *et al.*, 2001), and changes in the phosphorylation state of the LIC are correlated with changes in membrane association (Niclas *et al.*, 1996). Analysis of the *Chlamydomonas* LIC sequence indicates that it also contains several potential phosphorylation sites, and many seemed to be conserved in other D2LICs. An important next step will be to determine whether the *Chlamydomonas* LIC is phosphorylated, and if it is, how might the phosphorylation state of LIC vary between the cell body and the flagellar compartment, between the membrane plus matrix fraction and the axoneme-associated fraction (Figure 2), or in different mutant backgrounds (see below).

The central region of the *Chlamydomonas* LIC is most highly conserved with other members of the D1LIC and D2LIC family (Figure 1C). This region contains a RAS signature motif previously identified as a common feature of the LIC family (Figure 1C; Grissom *et al.*, 2002). The conserved region also includes domains identified as a cargo-binding site in rat D1LIC1 (Tynan *et al.*, 2000b) and a Rab4a interaction site in the human D1LIC sequence (Bielli *et al.*, 2001). These results suggest the possibility that the cDHC1b complex might be regulated by interaction with G proteins. Several G protein isoforms have previously been detected in *Chlamydomonas* flagella (Huber *et al.*, 1996), but whether they play a role in flagellar assembly is still unknown. Interestingly, a preliminary report has identified a raft particle protein, IFT27, as a Ras-like small G protein (cited in Rosen-

baum and Witman, 2002), but whether this protein interacts with the cDHC1b complex is not yet clear.

Another approach for the study of cDHC1b regulation is to screen the collection of flagellar mutants and identify those strains in which the distribution of the cDHC1b motor is altered. For example, the retrograde IFT mutants accumulate cDHC1b and the LIC in flagellar bulges (Figure 5; Iomini *et al.*, 2001), leading to the proposal that components of raft complex A play a role in regulating cDHC1b during IFT. We have identified the *lf* mutants as another group with an unusual cDHC1b/LIC phenotype. The cDHC1b/LIC complex accumulates at the tips of the long flagella along with all of the other IFT components (Figure 6). These observations are consistent with previous reports that *lf* mutants exhibit swellings filled with electron dense material at the tips of their flagella (McVittie, 1972). The accumulation of the cDHC1b/LIC complex and other IFT components at the distal tip is significant in light of recent work identifying this region as a key site for the regulation of IFT and flagellar assembly (Iomini *et al.*, 2001; Marshall and Rosenbaum, 2001). For instance, the flagellar tip is the site where antero-grade IFT particles are unloaded and remodeled into retro-grade IFT particles (Iomini *et al.*, 2001). The flagella tip is also the site where the cDHC1b motor must be activated for transport of retrograde particles back to the cell body. The accumulation of IFT components at the tips of the *lf* mutants therefore suggests that the *LF* gene products may function directly or indirectly to modulate cDHC1b activity and retrograde transport. We are currently isolating cDHC1b complexes from wild-type and *lf* mutant flagella to test this hypothesis. In addition, progress in the cloning of the *LF* loci should soon yield new information about the identities of the *LF* gene products and their potential roles in the regulation of the cDHC1b motor and retrograde IFT (Amundsen and Lefebvre, 1998; Asleson *et al.*, 1998).

Note added in proof. Since this manuscript was accepted for publication, another report localizing DHC2 and D2LIC in cilia of brain, retina, and cultured cells has appeared (Mikami, *et al.*, J. Cell Sci. [2002]. *115*, 4801–4808).

REFERENCES

Addinall, S.G., Mayr, P.S., Doyle, S., Sheehan, J.K., Woodman, P.G., and Allan, V.J. (2001). Phosphorylation by cdc2-cyclinB1 kinase releases cytoplasmic dynein from membranes. J. Biol. Chem. *276*, 15939–15944.

Afzelius, B.A. (1999). Asymmetry of cilia and of mice and men. Int. J. Dev. Biol. *43*, 283–286.

Alieva, I.B., Gorgidze, L.A., Komarova, Y.A., Chernobelskaya, O.A., and Vorobjev, I.A. (1999). Experimental model for studying the primary cilia in tissue culture cells. Membr. Cell Biol. *12*, 895–905.

Amundsen, C.D., and Lefebvre, P.A. (1998). *LF2*, A gene required for flagellar length control in *Chlamydomonas reinhardtii*. Mol. Biol. Cell (suppl) *9*, 396a.

Asleson, C.M., and Lefebvre, P.A. (1998). Genetic analysis of flagellar length control in *Chlamydomonas reinhardtii*: a new long-flagella locus and extragenic suppressor mutations. Genetics *148*, 693–702.

Aughsteen, A. (2001). The ultrastructure of primary cilia in the endocrine and excretory duct cells of the pancreas of mice and rats. Eur. J. Morphol. *39*, 277–283.

Barsel, S.-E., Wexler, D.E., and Lefebvre, P.A. (1988). Genetic analysis of long-flagella mutants of *Chlamydomonas reinhardtii*. Genetics *118*, 637–648.

Bielli, A., Thornqvist, P.O., Hendrick, A.G., Finn, R., Fitzgerald, K., and McCaffrey, M.W. (2001). The small GTPase Rab4A interacts with the central region of cytoplasmic dynein light intermediate chain-1. Biochem. Biophys. Res. Commun. *281*, 1141–1153.

Bonifacino, J.S., Dell'Angelica, E.C., and Springer, T.A. (1999). Immunoprecipitation. Curr. Prot. Protein Sci. *2*, 9.8.1–9.8.28.

Cole, D.G., Chinn, S.W., Wedaman, K.P., Hall, K., Vuong, T., and Scholey, J.M. (1993). Novel heterotrimeric kinesin-related protein purified from sea urchin eggs. Nature *366*, 268–270.

Cole, D.G., Diener, D.R., Himelblau, A.L., Beech, P.L., Fuster, J.C., and Rosenbaum, J.L. (1998). *Chlamydomonas* kinesin-II-dependent Intraflagellar transport (IFT): IFT particles contain proteins required for ciliary assembly in *Caenorhabditis elegans* sensory neurons. J. Cell Biol. *141*, 993–1008.

Criswell, P.S., and Asai, D.J. (1998). Evidence for four cytoplasmic dynein heavy chain isoforms in rat testis. Mol. Biol. Cell *9*, 237–247.

Criswell, P.S., Ostrowski, L.E., and Asai, D.J. (1996). A novel cytoplasmic dynein heavy chain: expression of DHC1b in mammalian ciliated epithelial cells. J. Cell Sci. *109*, 1891–1898.

Deane, J., Cole, D., Seeley, E., Diener, D., and Rosenbaum, J. (2001). Localization of intraflagellar transport protein IFT52 identifies basal body transitional fibers as the docking site for IFT particles. Curr. Biol. *11*, 1586–1590.

Dell, K.R., Turck, C.W., and Vale, R.D. (2000). Mitotic phosphorylation of the dynein light intermediate chain is mediated by cdc2 kinase. Traffic *1*, 38–44.

Gardner, L.C., O'Toole, E., Perrone, C.A., Giddings, T., and Porter, M.E. (1994). Components of a "dynein regulatory complex" are located at the junction between the radial spokes and the dynein arms in *Chlamydomonas* flagella. J. Cell Biol. *127*, 1311–1325.

Gibbons, B.H., Asai, D.J., Tang, W.J.Y., Hays, T.S., and Gibbons, I.R. (1994). Phylogeny and expression of axonemal and cytoplasmic dynein genes in sea urchins. Mol. Biol. Cell *5*, 57–70.

Gill, S.R., Cleveland, D.W., and Schroer, T.A. (1994). Characterization of DLC-A and DLC-B, two families of cytoplasmic dynein light chain subunits. Mol. Biol. Cell *5*, 645–654.

Goodenough, U.W., and Heuser, J. (1984). Structural comparison of purified dynein proteins with *in situ* dynein arms. J Mol. Biol. *180*, 1083–1118.

Grissom, P.M., Vaisberg, E.A., and McIntosh, J.R. (2002). Identification of a novel light intermediate chain (D2LIC) for mammalian cytoplasmic dynein 2. Mol. Biol. Cell *13*, 817–829.

Habermacher, G., and Sale, W. (1997). Regulation of flagellar dynein by phosphorylation of a 138-kD inner arm dynein intermediate chain. J. Cell Biol. *136*, 167–176.

Harrison, A., Olds-Clarke, P., and King, S.M. (1998). Identification of the t complex-encoded cytoplasmic dynein light chain Tctex1 in inner arm I1 supports the involvement of flagellar dyneins in meiotic drive. J. Cell Biol. *140*, 1137–1147.

Huber, H., Beyser, K., and Fabry, S. (1996). Small G proteins of two green algae are localized to exocytic compartments and to flagella. Plant Mol. Biol. *31*, 279–293.

Hughes, S.M., Vaughan, K.T., Herskovits, J.S., and Vallee, R.B. (1995). Molecular analysis of a cytoplasmic dynein light intermediate chain reveals homology to a family of ATPases. J. Cell Sci. *108*, 17–24.

Iomini, C., Babaev-Khaimov, V., Sassaroli, M., and Piperno, G. (2001). Protein particles in *Chlamydomonas* flagella undergo a transport cycle consisting of four phases. J. Cell Biol. *153*, 13–24.

King, S.M., Barbarese, E., Dillman, J.F.I., Patel-King, R.S., Carson, J.H., and Pfister, K.K. (1996). Brain cytoplasmic and flagellar outer arm dyneins share a highly conserved Mr 8,000 light chain. J. Biol. Chem. *271*, 19356–19366.

King, S.H., Bonilla, M., Rodgers, M.E., and Schroer, T.A. (2002). Subunit organization in cytoplasmic dynein subcomplexes. Protein Sci. *11*, 1239–1250.

King, S.M., and Patel-King, R.S. (1995). The M_r = 8,000 and 11,000 outer arm dynein light chains from *Chlamydomonas* flagella have cytoplasmic homologues. J. Biol. Chem. *270*, 11445–11452.

Kozminski, K.G., Beech, P.L., and Rosenbaum, J.L. (1995). The *Chlamydomonas* kinesin-like protein *F.L.A10* is involved in motility associated with the flagellar membrane. J. Cell Biol. *131*, 1517–1527.

Marshall, W.F., and Rosenbaum, J.L. (2001). Intraflagellar transport balances continuous turnover of outer doublet microtubules: implications for flagellar length control. J. Cell Biol. *155*, 205–214.

Marszalek, J., Ruiz-Lozano, P., Roberts, E., Chien, K., and Goldstein, L. (1999). Situs inversus and embryonic ciliary morphogenesis defects in mouse mutants lacking the KIF3A subunit of kinesin-II. Proc. Natl. Acad. Sci. USA *96*, 5043–5048.

McVittie, A. (1972). Flagellum mutants of *Chlamydomonas reinhardtii*. J. Gen. Microbiol. *71*, 525–540.

Mitchell, D.R., and Rosenbaum, J.L. (1985). A motile *Chlamydomonas* flagellar mutant that lacks outer dynein arms. J. Cell Biol. *100*, 1228–1234.

Murcia, N.S., Richards, W.G., Yoder, B.K., Mucenski, M.L., Dunlap, J.R., and Woychik, R.P. (2000). The oak ridge polycystic kidney (*orpk*) disease gene is required for left-right axis determination. Development *127*, 2347–2355.

Myster, S.H., Knott, J.A., O'Toole, E., and Porter, M.E. (1997). The *Chlamydomonas Dhc1* gene encodes a dynein heavy chain subunit required for assembly of the I1 inner arm complex. Mol. Biol. Cell *8*, 607–620.

Myster, S.H., Knott, J.A., Wysocki, K.M., O'Toole, E., and Porter, M.E. (1999). Domains in the 1α dynein heavy chain required for inner arm assembly and flagellar motility in *Chlamydomonas*. J. Cell Biol. *146*, 801–818.

Neesen, J., Koehler, M., Kirschner, R., Steinlein, C., Kreutzberger, J., Engel, W., and Schmid, M. (1997). Identification of dynein heavy chain genes expressed in human and mouse testis: chromosomal localization of an axonemal dynein gene. Gene *200*, 193–202.

Niclas, J., Allan, V.J., and Vale, R.D. (1996). Cell cycle regulation of dynein association with membranes modulates microtubule-based organelle transport. J. Cell Biol. *133*, 585–593.

Nonaka, S., Tanaka, Y., Okada, Y., Takeda, S., Harada, A., Kanai, Y., Kido, M., and Hirokawa, N. (1998). Randomization of left-right asymmetry due to loss of nodal cilia generating leftward flow of extraembryonic fluid in mice lacking K.IF3B. motor protein. Cell *95*, 829–837.

Pazour, G.J., Dickert, B.L., Vucica, Y., Seeley, E.S., Rosenbaum, J.L., Witman, G.B., and Cole, D.G. (2000). *Chlamydomonas* IFT88 and its mouse homologue, polycystic kidney disease gene *tg737*, are required for assembly of cilia and flagella. J. Cell Biol. *151*, 709–718.

Pazour, G.J., Dickert, B.L., and Witman, G.B. (1999). The DHC1b (DHC2) isoform of cytoplasmic dynein is required for flagellar assembly. J. Cell Biol. *144*, 473–481.

Pazour, G.J., Wilkerson, C.G., and Witman, G.B. (1998). A dynein light chain is essential for the retrograde particle movement of intraflagellar transport (IFT). J. Cell Biol. *141*, 979–992.

Perrone, C.A., Myster, S.H., Bower, R., O'Toole, E.T., and Porter, M.E. (2000). Insights into the structural organization of the I1 inner arm dynein from a domain analysis of the 1 dynein heavy chain. Mol. Biol. Cell *11*, 1–17.

Perrone, C.A., Yang, P., O'Toole, E., Sale, W.S., and Porter, M.E. (1998). The *Chlamydomonas* IDA7 locus encodes a 140-kDa dynein intermediate chain required to assemble the I1 inner arm complex. Mol. Biol. Cell *9*, 3351–3365.

Piperno, G., and Mead, K. (1997). Transport of a novel complex in the cytoplasmic matrix of *Chlamydomonas* flagella. Proc. Natl. Acad. Sci. USA *94*, 4457–4462.

Piperno, G., Siuda, E., Henderson, S., Segil, M., Vaananen, H., and Sassaroli, M. (1998). Distinct mutants of retrograde intraflagellar transport (IFT) share similar morphological and molecular defects. J. Cell Biol. *143*, 1591–1601.

Poole, C., Jensen, C., Snyder, J., Gray, C., Hermanutz, V., and Wheatley, D. (1997). Confocal analysis of primary cilia structure and colocalization with the Golgi apparatus in chondrocytes and aortic smooth muscle cells. Cell Biol. Int. *21*, 483–494.

Poole, C.A., Zhang, Z.J., and Ross, J.M. (2001). The differential distribution of acetylated and detyrosinated α-tubulin in the microtubular cytoskeleton and primary cilia of hyaline cartilage chondrocytes. J. Anat. *199*, 393–405.

Porter, M.E., Bower, R., Knott, J.A., Byrd, P., and Dentler, W. (1999). Cytoplasmic dynein heavy chain 1b is required for flagellar assembly in *Chlamydomonas*. Mol. Biol. Cell *10*, 693–712.

Porter, M.E., Knott, J.A., Myster, S.H., and Farlow, S.J. (1996). The dynein gene family in *Chlamydomonas reinhardtii*. Genetics *144*, 569–585.

Porter, M.E., Power, J., and Dutcher, S.K. (1992). Extragenic suppressors of paralyzed flagellar mutations in *Chlamydomonas reinhardtii* identify loci that alter the inner dynein arms. J. Cell Biol. *118*, 1163–1176.

Rosenbaum, J.L., Cole, D.G., and Diener, D.R. (1999). Intraflagellar transport: the eyes have it. J. Cell Biol. *144*, 385–388.

Rosenbaum, J.L., and Witman, G.B. (2002). Intraflagellar transport. Nat. Rev. Mol. Cell. Biol. *3*, 813–825.

Sanders, M.A., and Salisbury, J.L. (1995). Immunofluorescence microscopy of cilia and flagella. Methods Cell Biol. *47*, 163–169.

Schafer, J.C., Haycraft, C.J., Thomas, J.H., Yoder, B.K., and Swoboda, P. (2003). XBX-1 encodes a dynein light intermediate chain (DLIC) required for retrograde intraflagellar transport and cilia assembly in *C. elegans*. Mol. Biol. Cell *14*, 2057–2070.

Signor, D., Wedaman, K.P., Orozco, J.T., Dwyer, N.D., Bargmann, C.I., Rose, L.S., and Scholey, J.M. (1999a). Role of a class DHC1b dynein in retrograde transport of IFT motors and IFT raft particles along cilia, but not dendrites, in chemosensory neurons of living *Caenorhabditis elegans*. J. Cell Biol. *147*, 519–530.

Signor, D., Wedaman, K.P., Rose, L.S., and Scholey, J.M. (1999b). Two heteromeric kinesin complexes in chemosensory neurons and sensory cilia of *Caenorhabditis elegans*. Mol. Biol. Cell *10*, 345–360.

Sloboda, R.D. (2002). A healthy understanding of intraflagellar transport. Cell Motil. Cytoskeleton *52*, 1–8.

Swoboda, P., Adler, H.T., and Thomas, J.H. (2000). The RFX-type transcription factor DAF-19 regulates sensory neuron cilium formation in *C. elegans*. Mol. Cell *5*, 411–421.

Tanaka, Y., Zhang, Z.Z., and Hirokawa, N. (1995). Identification and molecular evolution of new dynein-like protein sequences in rat brain. J. Cell Sci. *108*, 1883–1893.

Taulman, P.D., Haycraft, C.J., Balkovetz, D.F., and Yoder, B.K. (2001). Polaris, a protein involved in left-right axis patterning, localizes to basal bodies and cilia. Mol. Biol. Cell *12*, 589–599.

Tucker, R.W., Pardee, A.B., and Fujiwara, K. (1979). Centriole ciliation is related to quiescence and DNA synthesis in 3T3 cells. Cell *17*, 527–535.

Tuxhorn, J., Daise, T., and Dentler, W.L. (1998). Regulation of flagellar length in *Chlamydomonas*. Cell Motil. Cytoskeleton *40*, 133–146.

Tynan, S.H., Gee, M.A., and Vallee, R.B. (2000a). Distinct but overlapping sites within the cytoplasmic dynein heavy chain for dimerization and for intermediate chain and light intermediate chain binding. J. Biol. Chem. *275*, 32769–32774.

Tynan, S.H., Purohit, A., Doxsey, S.J., and Vallee, R.B. (2000b). Light intermediate chain 1 defines a functional subfraction of cytoplasmic dynein which binds to pericentrin. J. Biol. Chem. *275*, 32763–32768.

Vaisberg, E.A., Grissom, P.M., and McIntosh, J.R. (1996). Mammalian cells express three distinct dynein heavy chains that are localized to different cytoplasmic organelles. J. Cell Biol. *133*, 831–842.

Vaughan, P.S., Leszyk, J.D., and Vaughan, K.T. (2001). Cytoplasmic dynein intermediate chain phosphorylation regulates binding to dynactin. J. Biol. Chem. *276*, 26171–26179.

Walther, Z., Vashishtha, M., and Hall, J.H. (1994). The *Chlamydomonas FLA10*gene encodes a novel kinesin-homologous protein. J. Cell Biol. *126*, 175–188.

Waters, M.G., Clary, S.O., and Rothman, J.E. (1992). A novel 115-kD peripheral membrane protein is required for intercisternal transport in the Golgi stack. J. Cell Biol. *118*, 1015–1026.

Wheatley, D., Feilen, E., Yin, Z., and Wheatley, S. (1994). Primary cilia in cultured mammalian cells: detection with an antibody against detyrosinated α-tubulin (ID5) and by electron microscopy. J. Submicrosc. Cytol. Pathol. *26*, 91–102.

Wheatley, D., Wang, A., and Strugnell, G. (1996). Expression of primary cilia in mammalian cells. Cell Biol. Int. *20*, 73–81.

Wicks, S.R., de Vries, C.J., van Luenen, H.G.A.M., and Plasterk, R.H.A. (2000). CHE-3, a cytosolic dynein heavy chain, is required for sensory cilia structure and function in *Caenorhabditis elegans*. Dev. Biol. *221*, 295–307.

Yamazaki, H., Nakata, T., Okada, Y., and Hirokawa, N. (1995). KIF3A/3B: a heterotrimeric kinesin superfamily protein that works as a microtubule plus end-directed motor for membrane organelle transport. J. Cell Biol. *130*, 1387–1399.

Yang, P., and Sale, W.S. (2000). Casein kinase I is anchored on axonemal doublet microtubules and regulates flagellar dynein phosphorylation and activity. J. Biol. Chem. *275*, 18905–18912.

Yoder, B.K., Hou, X., and Guay-Woodford, L.M. (2002). The polycystic kidney disease proteins, polycystin-1, polycystin-2, polaris, and cystin, are co-localized in renal cilia. J. Am. Soc. Nephrol. *13*, 2508–2516.

Yoder, J.H., and Han, M. (2001). Cytoplasmic dynein light intermediate chain is required for discrete aspects of mitosis in *Caenorhabditis elegans*. Mol. Biol. Cell *12*, 2921–2933.